Flow Cytometry As a Novel Tool to Evaluate and Separate Vesicles Using Characteristic Scatter Signatures

Giddi Hema Sagar,[†] Manu D. Tiwari,[‡,§] and Jayesh R. Bellare*[,†,‡,§]

Department of Chemical Engineering, Department of Biosciences and Bioengineering, and Center for Research in Nanotechnology and Science, IIT Bombay, Mumbai- 400076, India

Received: March 26, 2010; Revised Manuscript Received: June 19, 2010

Vesicles are usually characterized for their structure by microscopy or, less often, by the addition of fluorescent dyes in a flow cytometer. We present a new method of studying these structures and associated forms by forward and side scatter analysis on a flow cytometer which has the advantage of simultaneous handling of large population of vesicles to identify their shapes and lamellarities. The technique is suitable for several types of vesicular structures like Multivesicular vesicles (MVV), multilamellar and unilamellar vesicles. Characteristic signatures are given by tubular structures and fine features thereon allow detection of complex structures such as fused and ellipsoidal forms. Coexistence of tubular and spherical structures, such as those known to form when surfactants/salt solutions are diluted, can clearly be detected by the signature pattern, which separates into two distinctly identifiable populations. The population can be sorted or separated easily based on these signatures and such sorting has allowed us to confirm our findings by microscopic observations. This novel method can thus be used for concurrent observations of vesicle populations with dye or more advantageously without employing any fluorescent tag.

Introduction

Vesicles are microstructures formed as a result of spontaneous emulsification of two immiscible systems. Due to the random nature of this process, a variety of structures are observed, differing, primarily, in their size and lamellarity.[1] Accordingly, they can be characterized as Multi- or Uni- lamellar vesicles[2] (MLVs and ULVs), Multivesicular vesicles (MVVs),[3] or Tubular vesicles. These microstructures find manifold applications in the fields of drug delivery, food industry, material synthesis, and oil recovery, among others.[4−6] One of the major sources of these vesicular structures is the surfactant−water system. Anionic, cationic as well as nonionic surfactants have been utilized for this purpose.[7−10]

The primary and most utilized method for observing vesicular microstructures has been optical microscopy. Size and lamellarity are the two most common parameters that are analyzed for microstructures; however, size correlations are difficult to perform, especially if the sample is polydisperse and the determination of the exact number of lamellae in a vesicle also poses its own challenges. In addition, different populations are difficult to be identified since simultaneous analysis of the complete sample is not possible. Reported methods for analyzing sizes of these microstructures include coulter counter and light microscopy (for particles greater than 1 μm), size exclusion chromatography, dynamic light scattering and electron microscopy (particles smaller than 0.2 μm), and flow cytometry (intermediate range).[11−17]

Flow cytometry is currently a widely used method for analyzing cell and particle behavior under flow conditions. In the case of vesicular microstructures, this method has been used for characterizing size distribution and internal aqueous volume of liposomes.[18] It is necessary in such studies to employ a fluorescent molecule to measure the vesicle size.[19,20] We thought it would be interesting to analyze the vesicle behavior with regard to their physical structure without any fluorescent tag on a flow cytometer. Signals corresponding to the side and the forward scatter correlate with internal complexity (lamellarity) and size of the vesicle populations, respectively. A comparison of information available from current approaches and our approach for studying vesicular microstructures is presented in Table 1.

To our knowledge, this is the first report of simultaneous analysis of vesicle shape and lamellarity without the use of any fluorescent molecule using flow cytometry. We have used the AOT−water mixture which is a well-recognized system for the production of vesicle structures[21] for our studies. These structures are known to exist in equilibrium as well as nonequilibrium states such as myelins.[22−24]

Methods

MLVs were prepared by dissolving a known concentration of Sodium dioctyl sulfosuccinate (AOT) in DI water followed by shearing at a constant shear rate for 1 day. The samples were then aged for 2−3 months. Dilutions of MLVs were prepared from the mother solution (prepared above) by adding known amounts of DI water and equilibrated for a week before analysis. ULV suspension was prepared at low surfactant concentration.

Polystyrene beads (Polybead Polystyrene) of known diameters (2.0 ± 0.024 μm, 6.0 ± 0.451 μm, 10.0 ± 0.37 μm, 25.0 ± 3.7 μm) were obtained from Polysciences Inc. (PA, USA) and were used to obtain a standard dot plot on the flow cytometer.

Flow cytometry analyses were carried out on a BD FACSAria instrument equipped with 488 nm (blue) laser and FSC, SSC detectors. The flow was through a 70-μm nozzle and sheath

* To whom correspondence should be addressed. Present address: Silicate Technology Lab, Department of Chemical Engineering, IIT Bombay, Mumbai-400076, India. Phone +91 22 25764217, Fax: +91 22 25726895, Email: jb@iitb.ac.in.

[†] Department of Chemical Engineering, IIT Bombay.

[‡] Department of Biosciences and Bioengineering, IIT Bombay.

[§] Center for Research in Nanotechnology and Science, IIT Bombay.

10.1021/jp1027433
Published on Web 07/21/2010

TABLE 1: Traditional and Current Approaches for Studying Vesicular Structures and Their Merits/Demerits

parameter	microscopy	current approach (flow cytometry with fluorescent dye)	our approach (flow cytometry without any dye)
dye	works with as well as without dye	needed	not required
scope	individual frames	simultaneous analysis of large populations	simultaneous analysis of large populations
statistics	poor	good	good
size distribution	visual only	relative sizing of populations possible	relative sizing of populations possible
shape analysis	visual only	limited	identification of shapes
structural complexity	visual only	limited	elucidation of relative structural complexity possible

pressure was maintained at 70 psi. The instrument was calibrated with Accudrop beads (BD Biosciences) for adjusting the drop delay value during sorting. For all studies, 10 000 events were recorded. Data were acquired and analyzed by the BD FACS-Diva software provided by the manufacturer. Sorted samples were also examined with the same optical microscope as stated below.

Optical micrographs were obtained on an inverted Confocal Laser Scanning Microscope (Olympus-IX81 FV500) with 60× and 20× objectives.

Results and Discussion

The FSC-SSC dot plot of a solution containing a mixture of polystyrene beads of known sizes (2.0 ± 0.024 μm, 6.0 ± 0.451 μm, 10.0 ± 0.37 μm, 25.0 ± 3.7 μm) is shown in Figure 1. It can be inferred that a variation in the size is directly correlated with an increase in the FSC signal since the forward scatter increases with increase in the diameter of the beads. Further, the SSC-signal also marginally increases with size which is attributable to the increase in relative complexity with size. All the other beads, except the 25.0 ± 3.7 μm beads, are visible as fairly distinct populations. The 25.0 ± 3.7 μm beads, however, present an elongated population which can be attributed to their high standard deviation.

The FSC-SSC dot plots for different surfactant concentrations are shown in Figure 2 along with their corresponding optical micrographs. It is well-known that with variations in surfactant concentration, the size and lamellarity of vesicles undergoes defined changes.[16,21,22] As observed in Figure 2a for 2% AOT, a polydisperse vesicle population is present in the mixture, containing mostly multilamellar structures. Upon close observation, two populations can be seen which differ considerably in their side scatters and thence, their lamellarities. This is further substantiated by the presence of two population centers in the corresponding contour plot (not shown).

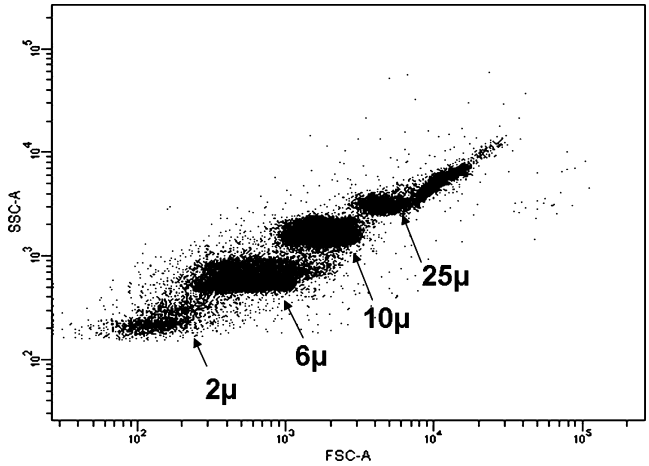

Figure 1. Forward and side-scatter dot plot of a solution containing a mixture of polystyrene beads of known sizes.

In order to fully confirm the presence of two populations, microscopy was performed. As seen in Figure 2 (right panel), two distinct lamellar populations are present which differ in their sizes. The higher scatter can, thus be attributed to the presence of complex structures- single and multivesicular vesicles.

An increase in the surfactant concentration leads to the formation of more MLVs, which are more homogeneous in terms of their forward and side scatters and, thus, in their sizes and lamellarities. This is exhibited in the case of to 8% surfactant (Figure 2b) which causes production of more MLVs (presumably due to the rupture of multivesicular vesicles) which are still smaller in size as compared to the parent population. In addition, fused structures also probably exist as evidenced by the presence of a distinct population as a tail in the dot plot. An almost uniform population in the micrograph with a lower percentage of complex structures is established. Finally, increasing the surfactant concentration to 16% (Figure 2c) leads to the production of an almost homogeneous MLV population with a low side scatter. This is in conformity with the general observation that homogeneous concentrated MLV populations exist at about 16% surfactant which is exhibited in the micrograph.[16]

Surfactant concentrations <1% produce a typical profile on the FSC-SSC dot plot in the form of a flattened S-shaped curve as shown in Figure 3. It is known from literature that a diagonal line on the FSC-SSC dot plot corresponds to tubular and comma-shaped structures.[25,26] In our experiments, we observed events along a diagonal indicating the presence of such structures (Figure 3a). This characteristic signature is found to repeat itself under different conditions of salt/surfactant concentrations (discussed later) and to our knowledge is the first such report.

Microscopic observations for these samples establish the presence of tubular and comma-shaped structures (Figure 3, right panel). Apart from these fused, ellipsoidal, 8-shaped and aggregated structures are also seen. The probable reason for the repeated appearance of the straight part of the signature is due to regular tubular forms while the bends in the pattern could arise because of the other complex structures mentioned above. From this, it can be envisaged that a decrease in the surfactant concentration would reduce the complexity of the structures formed. Indeed, this appears to be the case as evident by the evanescence of the signature at lower surfactant concentrations

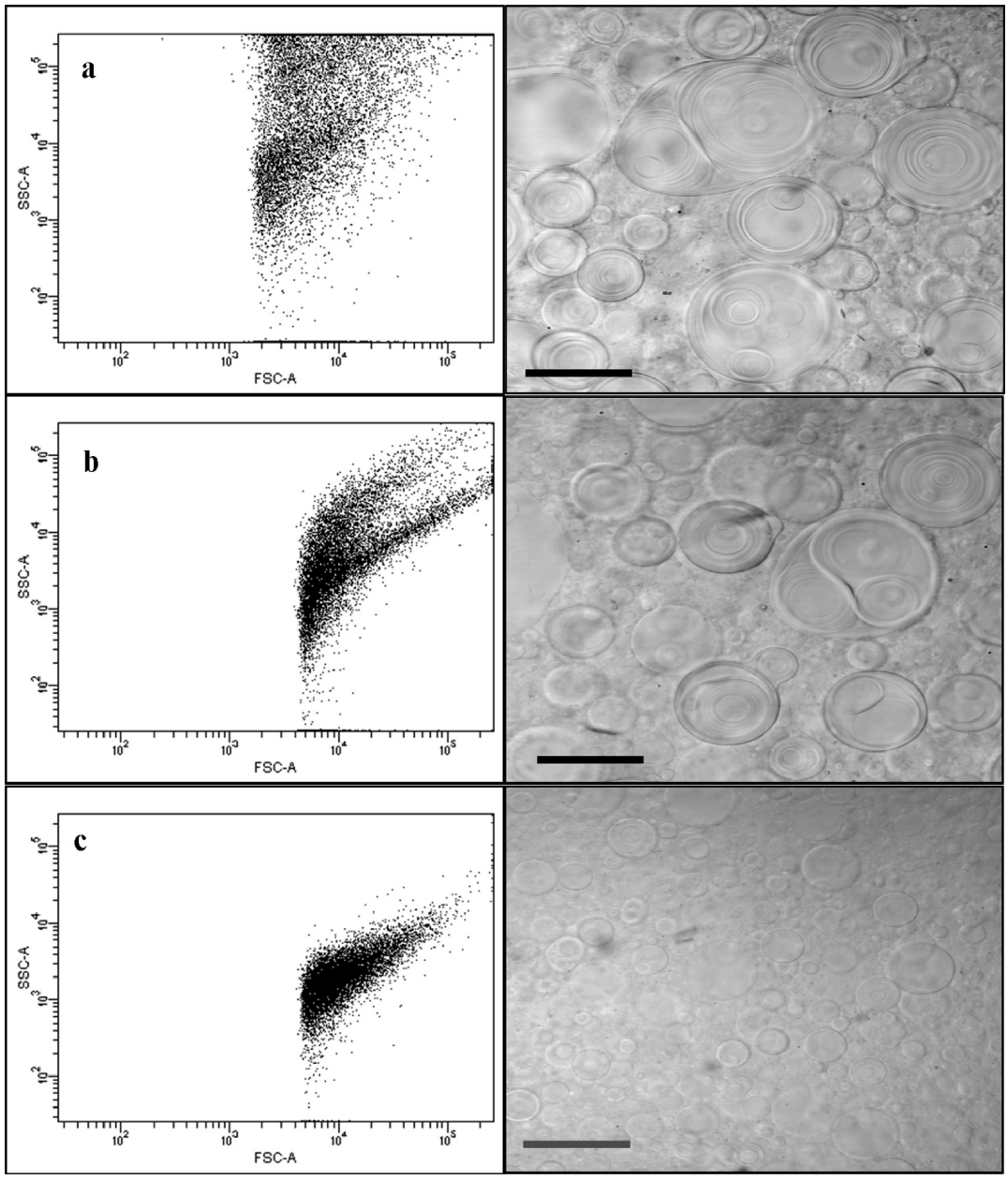

Figure 2. Forward and side-scatter dot plots (left) and optical micrographs (right) of MLVs. Arrows indicate populations differing in their sizes and lamellarities. (a) 2% AOT; (b) 8% AOT; (c) 16% AOT. Scale bar represents 50 μm.

(Figure 3b,c) and the emergence of a mixed population of ellipsoidal and spherical structures that are largely unilamellar.

Figure 4 shows the dot plot and micrograph of a ULV suspension. As expected, it exhibits reduced side and forward scatters when compared with the MLV samples. This occurs because ULVs are considerably less complex vis-à-vis their lamellarity when compared to MLVs. Also, the ULV population is not as dense as observed for the MLVs and is actually "spread out" in the dot plot. This is attributable to the presence of different sized ULVs and low sized MLV in the suspension. A tailed population in the dot plot indicates the existence of aligned structures.

On the basis of the foregoing observations, we performed further experiments to analyze the effects of NaCl/AOT concentrations. It is already known that tubular structures exist for certain ratios of NaCl/AOT concentrations.[16,27,28] We used NaCl at 25, 50, 100, and 300 mM for 1% AOT first and also for 2%, 3%, and 4% AOT. We present results for 1% and 4% (Supporting Information) as the illustrative ones.

Scatter dot plots for 1% AOT at 25 mM and 50 mM NaCl are presented in Figure 5. An S-shaped pattern suggests the presence of tubular structures which is confirmed by microscopic observations. The reappearance of this signature pattern further confirms the existence of tubular and other complex structures at low salt concentration. This "signature", however, has lesser density in its "tail" as compared to that of pure MLVs suggesting a lower percentage of complex structures. An increase in the salt concentration from 25 to 100 mM (Figure 6) leads to emergence of a new population and the disappearance of the "signature" pattern. This new population becomes clearly distinct as the salt concentration is further increased to 300 mM (P2 in Figure 6b) and has a lower side scatter, which suggests a decrease in the lamellarity.

These findings are in contrast to that of pure MLVs since the signature does not precede emergence of newer populations, thus, highlighting the role played by salt. Presumably, NaCl acts as a stabilizing agent for the newly formed smaller structures and leads to their accumulation, which is not possible

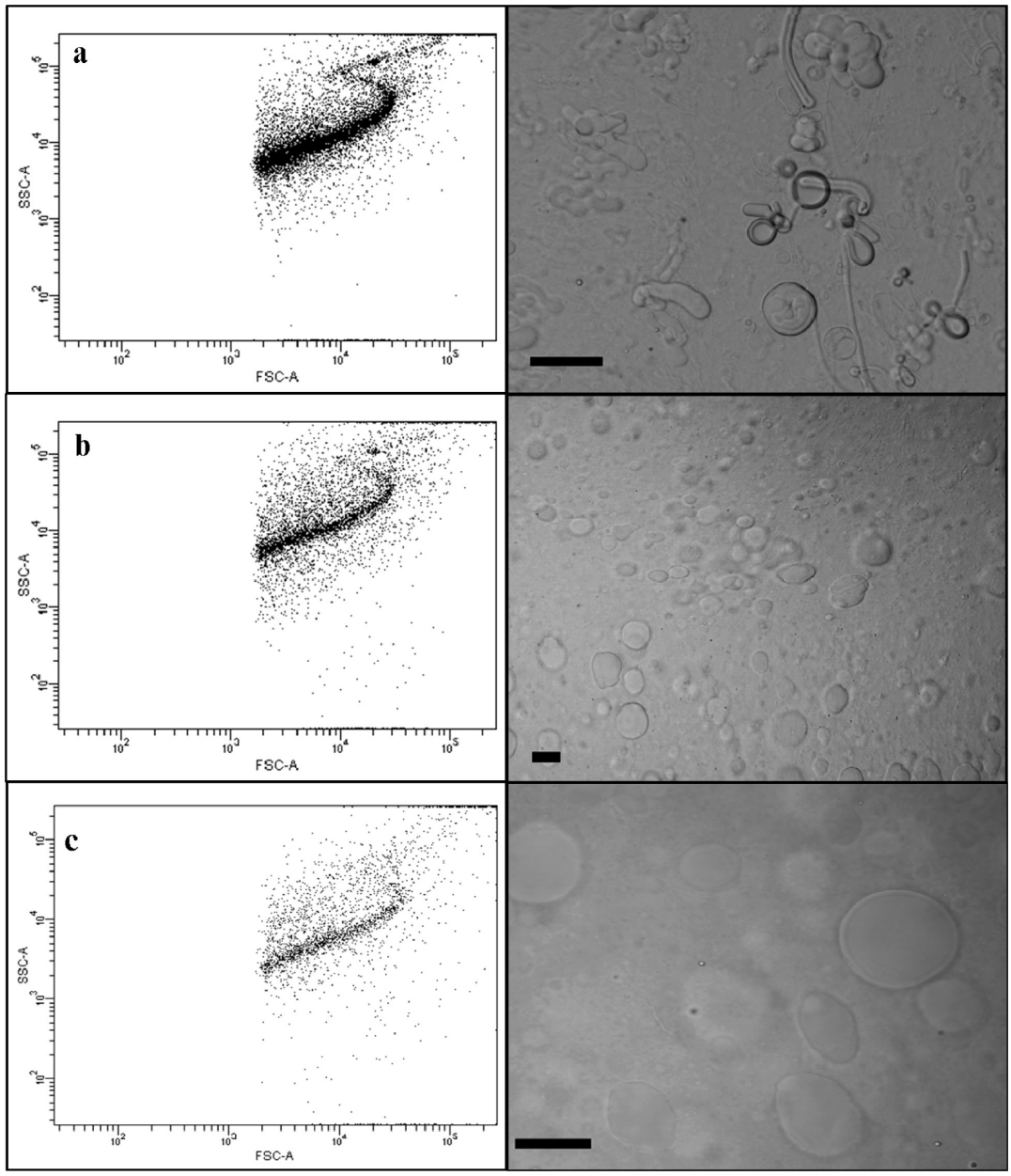

Figure 3. A closer look at the "signature" pattern of MLV figures; Parts a, b, and c are AOT concentrations at 0.5%, 0.05%, and 0.005%, respectively. Scale bar represents 20 μm.

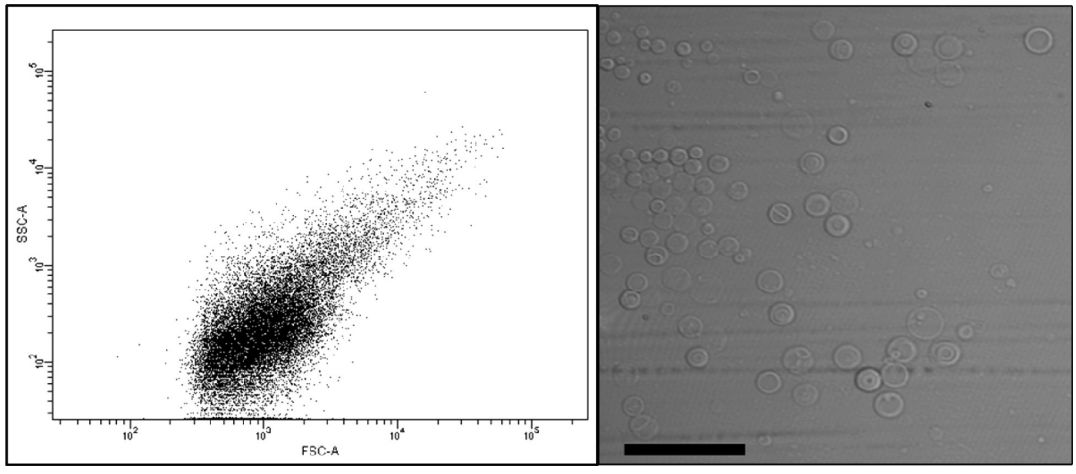

Figure 4. Forward and Side-scatter dot plot (left) and optical micrograph (right) of ULV suspension. Scale bar represents 100 μm.

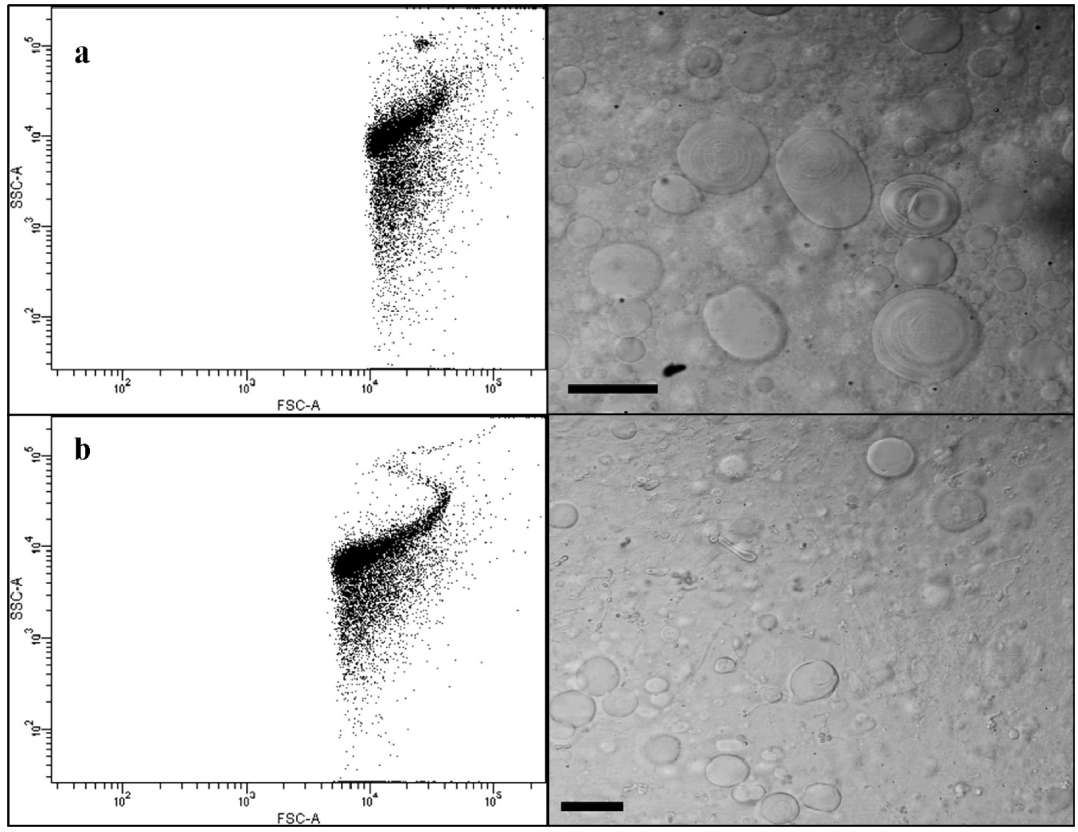

Figure 5. Scatter dot plots and micrographs of surfactant-salt mixtures. (a) 1% AOT-25 mM NaCl; (b) 1% AOT-50 mM NaCl. Scale bar represents 50 μm.

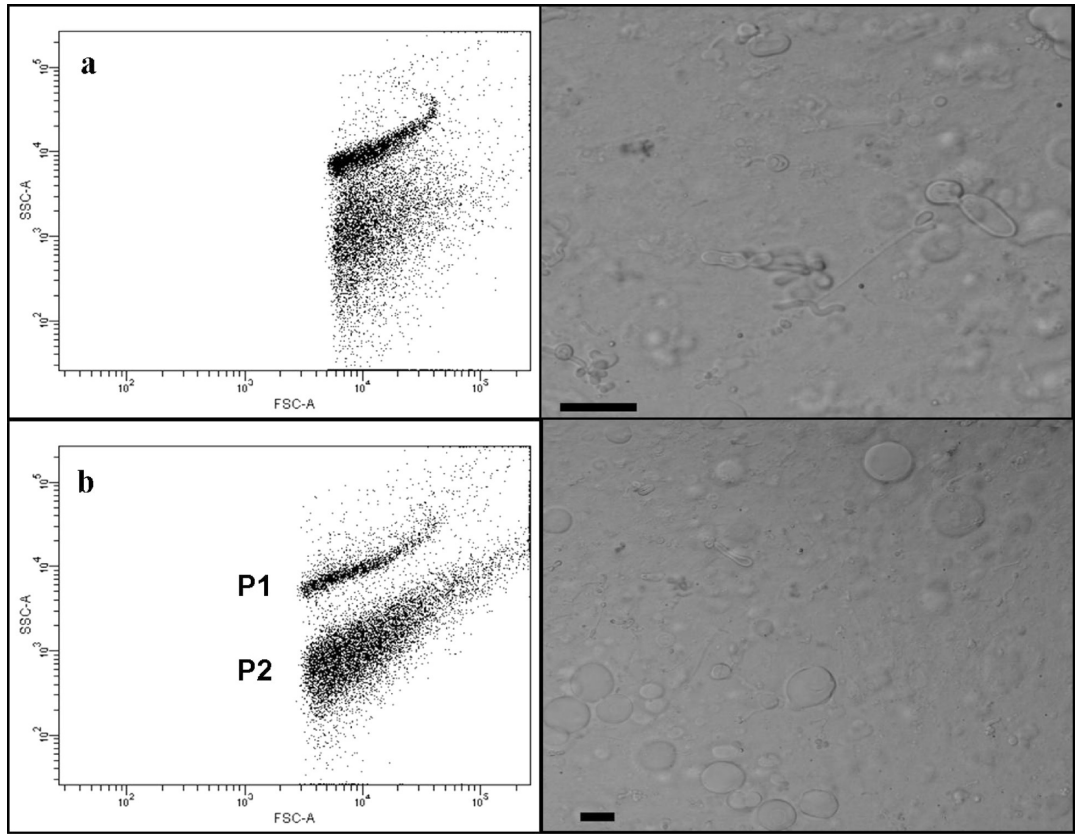

Figure 6. Scatter dot plots and micrographs of surfactant-salt mixtures. (a) 1% AOT-100 mM NaCl; (b) 1% AOT-300 mM NaCl. Scale bar represents 20 μm.

with water only. Scatter dot plots for 4% AOT/salt solutions are shown in Supporting Information. Here too, a similar behavior is observed, that is, disappearance of the signature followed by appearance of a new population. This is a novel

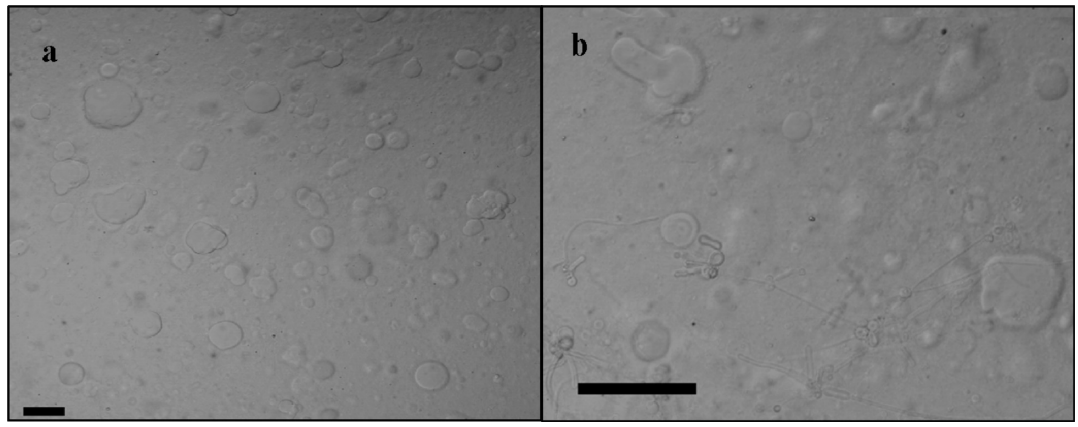

Figure 7. Micrographs of MLV populations (1% AOT-300 mM NaCl) after sorting. (a) P2 (Lower population in Figure 4b); (b) P1 (Upper population in Figure 4b). Scale bar represents 20 μm.

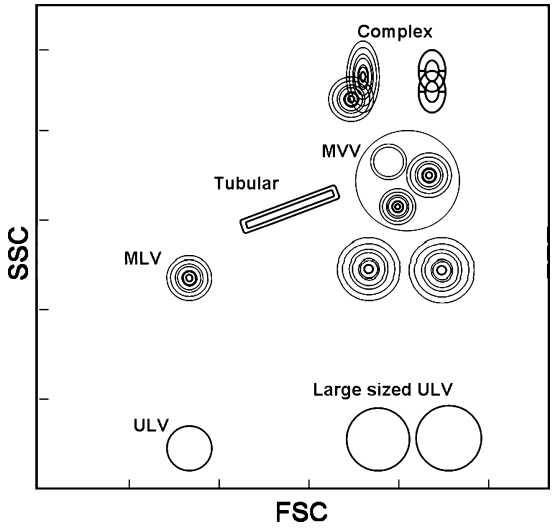

Figure 8. Scatter regions associated with different types of surfactant vesicles.

finding indicating that upon change in the osmolality of the solution, a pre-existing population gives rise to a new population which is less complex than the parent thereby confirming that the salt is a major steadying factor for maintaining the newly formed structures as distinct entities.

Due to their characteristic signatures, we were able to sort the two distinct populations at 1% AOT/300 mM NaCl on a flow cytometer and observed the sorted populations microscopically (Figure 7). As expected, the lower population (P2) is considerably less complex in terms of MLV shapes as compared to the upper population (P1) which exhibits tubular structures. It can thus be envisaged that addition of salt nucleates the formation of novel MLV structures; when this salt concentration is high enough, it stabilizes these entities which then emerge as distinct populations on the scatter dot plot.

The segmentation in the dot plot arises from angular distribution of intensities which is explained by the Mie theory,[29] and which the FACS instrument measures at a fixed angle. For a homogeneous population with known exact geometry and complexity, this scatter distribution can be calculated from Mie theory but the inverse problem does not give a single valued solution. Hence, each type of colloid with its given geometry and complexity would need a calibration to be performed as a prelude to its study by flow cytometry, as was done in the current work.

The method, thus, is suitable for physical separation of MLV populations and can have widespread applications in fields such as drug delivery where size-based fractionation of MLV populations is essential in improving the efficacy of the formulation. The experimental observations, presented in this work, permit us to outline the regions on a dot plot associated with the scatter signals (FSC and SSC) of different vesicle types as shown in Figure 8. Further, as illustrated in Table 1, our approach to the study of MLVs permits concurrent population analyses and provides useful insights into the shapes and relative sizes of these populations. Furthermore, the roles played by stabilizers and excipients in equilibrating the MLV populations are brought to the fore which is not possible with the current methods of studying MLVs. This can aid us in understanding the mechanism of formation and stabilization of these microstructures.

Conclusions

Vesicle structures have been analyzed by flow cytometry using forward and side scatter analysis without any fluorescent tags. Multilamellar and Unilamellar vesicles are detected as distinct populations on the dot plot. Changes in the lamellarity and size of the vesicles lead to corresponding shifts on the dot plots. A "signature" pattern has been identified at low surfactant concentrations indicating the presence of tubular and complex structures which are confirmed by microscopic observations. Effect of NaCl on the physical structure of vesicles has also been studied which indicates the emergence of a new population that is stable enough to be detected as a distinct signal on the scatter plot thus highlighting the stabilizing effect of salt. This pattern is repeated across different AOT concentrations.

Thus, apart from detecting vesicle structures without the need of any fluorescent tags, flow cytometry can be used to decipher their physical states vis-à-vis shape, size, and complexity and monitor the emergence of different populations. The method can be applied to physically separate the detected populations and to study the evolution of MLV structures with different excipients.

Acknowledgment. The authors thankfully acknowledge the use of Flow Cytometry Central Facility at CRNTS, IIT Bombay.

Supporting Information Available: Figure S1. Scatter dot plots of surfactant-salt mixtures. (a) 4% AOT-25 mM NaCl; (b) 4% AOT-50 mM NaCl; (c) 4% AOT-300 mM NaCl. This material is available free of charge via Internet at http://pubs.acs.org.

References and Notes

(1) Gradzielski, M. J. *Phys. Condens. Matter* **2003**, *15*, 656.

(2) Kaler, E. W.; Murthy, A. K.; Rodriguez, B. E.; Zasadzinski, J. A. *Science* **1989**, *245*, 1371.
(3) Tresset, G.; Takeuchi, S. *Anal. Chem.* **2005**, *77*, 2795.
(4) Torchilin, V. P. *Nat. Rev. Drug Disc.* **2002**, *4*, 145.
(5) Svenson, S. *Curr. Opin. Colloid Interface Sci.* **2004**, *9*, 201.
(6) Uchegbu, I. F.; Vyas, S. P. *Int. J. Pharm.* **1998**, *172*, 33.
(7) Moenkkoenen, J.; Urtti, A. *Adv. Drug Delivery Rev.* **1998**, *34*, 37.
(8) Limin, Z.; Ganzuo, L.; Zhiwei, S. *Colloids Surf. A* **2001**, *190*, 275.
(9) Murthy, K.; Easwar, N.; Singer, E. *Colloid Polym. Sci.* **1998**, *276*, 940.
(10) Danino, D.; Weihs, D.; Zana, R.; Oraedd, G.; Lindblom, G.; Abe, M.; Talmon, Y. *J. Colloid Interface Sci.* **2003**, *259*, 382.
(11) Woodle, M. C.; Papahadjopoulos, D. *Methods Enzymol.* **1989**, *171*, 193.
(12) Harris, J. K.; Rose, G. D.; Bruening, M. L. *Langmuir* **2002**, *18*, 5337.
(13) Almgren, M.; Edwards, K.; Karlsson, G. *Colloids Surf. A* **2000**, *174*, 3.
(14) Jederström, G.; Russell, G. *J. Pharm. Sci.* **2006**, *70*, 874.
(15) Hupfeld, S.; Holsaeter, A. M.; Skar, M.; Frantzen, C. B.; Brandl, M. *J. Nanosci. Nanotechnol.* **2006**, *6*, 3025.
(16) Segota, S.; Tezak, D. *Adv. Colloid Interface Sci.* **2006**, *121*, 51.
(17) Fuller, R. R.; Sweedler, J. V. *Cytometry* **1996**, *25*, 144.
(18) Sato, K.; Obinata, K.; Sugawara, T.; Urabe, I.; Yomo, T. *J Biosc. Bioeng.* **2006**, *102*, 171.
(19) Toyota, T.; Takakura, K.; Kageyama, Y.; Kurihara, K.; Maru, N.; Ohnuma, K.; Kaneko, K.; Sugawara, T. *Langmuir* **2008**, *24*, 3037.
(20) Nishimura, K.; Hosoi, T.; Sunami, T.; Toyota, T.; Fujinami, M.; Oguma, K.; Matsuura, T.; Suzuki, H.; Yomo, T. *Langmuir* **2009**, *25*, 10439.
(21) Bergenholtz, J.; Wagner, N. J. *Langmuir* **1996**, *12*, 3122.
(22) Buchanan, M.; Arrault, J.; Cates, M. E. *Langmuir* **1998**, *14*, 7371.
(23) Dave, H.; Surve, M.; Manohar, C.; Bellare, J. *J. Colloid Interface Sci.* **2003**, *264*, 76.
(24) Haran, M.; Chowdhury, A.; Manohar, C.; Bellare, J. *Colloids Surf. A* **2002**, *205*, 21.
(25) Vassilopoulos, A.; Wang, R. H.; Petrovas, C.; Ambrozak, D.; Koup, R.; Deng, C. *Int. J. Biol. Sci.* **2008**, *4*, 133.
(26) Schmid, S. A.; Gaumanna, A.; Wondraka, M.; Eckermann, C.; Schultec, S.; Klieser, W.; Wheatley, D. N.; Schughart, L. A. *Exp. Cell Res.* **2007**, *313*, 2531.
(27) Zemb, T.; Dubois, M.; Deme, B.; Gulikkrzywicki, T. *Science* **1999**, *283*, 816.
(28) Oda, R.; Huc, I.; Schmutz, M.; Candau, S. J.; Mackintosh, F. C. *Nature* **1999**, *399*, 566.
(29) Bohren, C. F.; Huffman, D. R. *Absorption and Scattering of Light by Small Particles*; Wiley-VCH: Weinheim, 2004.

JP1027433